RSC Advances

PAPER

View Article Online
View Journal | View Issue

Cite this: *RSC Adv.*, 2021, **11**, 7043

Versatile one-pot synthesis of gold nanoclusters and nanoparticles using 3,6-(dipyridin-2-yl)-(1,2,4,5)-tetrazine†

Yahdi Bin Rus,[a] Margarita Bosmi,[a] Stéphane Maisonneuve,[a] Vincent Guérineau,[b] Vincent Noël,[c] Alexa Courty[d] and Fabien Miomandre *[a]

Received 31st December 2020
Accepted 1st February 2021

DOI: 10.1039/d0ra10961d

rsc.li/rsc-advances

A one-pot synthesis of gold nano-objects is described by simply mixing a gold salt ($HAuCl_4$), dodecanethiol and 3,6-di-2-pyridyl-1,2,4,5-tetrazine. When a large excess of thiol is used, gold nanoclusters of 2 nm are obtained in a large amount and with a narrow size distribution. The reaction mechanism was investigated by absorption and emission spectroscopies and shows the *in situ* formation of dihydrotetrazine acting as the reductant of Au(III) to make Au(0). Au nanoclusters were isolated from the molecular precursors by HPLC. The nature of the ligands stabilizing Au nanoclusters was investigated by various techniques such as mass spectrometry, SEM-EDS, XPS and NMR. Thiol and tetrazine are shown to play both the role of ligand stabilizing the clusters. Finally, when a much smaller amount of thiol is used, a mixture of Au nanoclusters and Au nanoparticles of 10–15 nm, sometimes aggregated into clusters of 50 nm is obtained. The formation of larger nanoobjects is explained by the lower amount of thiol available to block the growth at the early stage as shown by UV-vis absorption monitoring.

Introduction

Gold nanoparticles (NP) have attracted the interest of the scientific community for a long time now due to their peculiar optical properties[1] which offer a large panel of applications in biotechnology,[2] medicine,[3] sensing,[4] catalysis[5] among others. Their synthesis is known since the pioneering work of Faraday in the 19th century and made possible at large scale using mainly either Turkevich[6] (in water) or Brust-Schiffrin[7] (in organic solvent) protocols. Based on the work of Brust, it appears that slight adjustments in the protocols, in particular increasing the ligand *vs.* gold ratio, led to the synthesis of ultra-small nanoparticles called metal protected clusters (MPC),[8] usually coated with thiolates. This further step allowed researchers to play at the boundary between nano-objects behaving like large molecules with defined size and mass and those with quantum size properties like plasmon resonance. It is now acknowledged that this boundary lies in terms of particle size near 2 nm diameter: below is the field of nanoclusters with molecular-type properties whereas above is the domain of nanoparticles.[9] One of the difficulties to overcome in the synthesis of nanoclusters is polydispersity,[10] which sometimes requires additional steps of fractionation to get well defined sizes. Murray *et al.* demonstrated two decades ago the possibility to get directly well-defined sizes down to 1.8 nm using dodecanethiol.[11] One-pot syntheses of gold nanoclusters (NC) of various sizes have been the subject of many publications since then, due to the easiness of their use. Two kinds of processes have emerged, a bottom-up starting from gold salts or gold complexes and a top-down consisting in etching nanoparticles by addition of an excess of ligands or by phase transfer.[12] Most of these syntheses rely on the use of mild reductants like citrate, ascorbate,[13] hydrazine hydrate,[14] borohydride[15,16] among others, added to the solution of gold salt with a surfactant (alkanethiols,[17–19] phosphines,[20] BSA,[21] DNA,[22] …) to stabilize the nano-objects formed. In some cases, the same moiety can act both as the surfactant and the reducing agent.

Another strategy of interest consists in generating the reductant *in situ*. This has the advantage of starting with very stable products, totally non-sensitive to the presence of residual oxygen in the solution and thus limits side-reactions leading to a narrower size distribution of the final nano-objects. The method presented in this paper uses an *in situ* prepared reductant, namely a dihydrotetrazine derivative, obtained from the reduction of the parent tetrazine by dodecanethiol (DDT). This method is inspired from the work of Biswas *et al.* who demonstrated for the first time the possibility of using a dihydrotetrazine as the reductant of a metallic salt to make metallic nanoparticles, but with a large size distribution around an

[a]Université Paris-Saclay, ENS Paris-Saclay, CNRS, PPSM, 4 Avenue des Sciences, 91190 Gif-sur-Yvette, France. E-mail: mioman@ens-paris-saclay.fr

[b]Université Paris-Saclay, CNRS, Institut de Chimie des Substances Naturelles, UPR2301, 91198 Gif-sur-Yvette, France

[c]Université de Paris, CNRS, ITODYS, 15 rue Jean de Baïf, 75013 Paris, France

[d]Sorbonne Université, CNRS, MONARIS, 4 place Jussieu, 75005 Paris, France

† Electronic supplementary information (ESI) available. See DOI: 10.1039/d0ra10961d

average diameter of 12 nm.[23] In addition, the same author showed that 3,6-dipyridin-2-yl-1,2,4,5-tetrazine (bptz, see Scheme 1) was able to oxidize alkanethiols into disulfide.[24] Based on these results, we propose a new one-pot synthesis of gold nanoparticles by mixing a gold salt (chloroauric acid), an alkanethiol (DDT) and 3,6-di(pyridyn-2-yl)-1,2,4,5-tetrazine (bptz) in ethanol, leading to Au nanoclusters(NCs) or nanoparticles(NPs) according to the proportions. Besides, bptz is a well-known reagent for cycloaddition through inverse demand Diels–Alder reaction[25,26] and a couple of examples highlight this role to functionalize nanoparticles.[27,28] Thus its use in synthesizing and possibly capping gold nanoparticles opens the way to post-grafting on carbonaceous materials like carbon nanotubes[29] or graphene. Prior to that, we need to elucidate precisely the mechanism of the nano-object formation and the role played by each component, which is the topic of the present investigation.

Results and discussion

Our investigation is divided in two sections, since two kinds of nano-objects are obtained according to the experimental conditions.

A. Gold nanoclusters

A.1 Synthesis. 2 mg (5 μmol) of $HAuCl_4 \cdot 3H_2O$ were dissolved in 8 mL of absolute ethanol. Under stirring, 3 mL (12.5 mmol) of 1-dodecanethiol (DDT) is added slowly to the previous solution. Separately, 6 mg (25.3 μmol) of 3,6-di-2-pyridinyl-1,2,4,5-tetrazine (bptz) are dissolved in 2 mL of absolute ethanol and stirred for 30 minutes. Under rapid stirring, the bptz solution is then added dropwise to the $HAuCl_4$ + DDT one. The reaction takes place at room temperature, and is kept under 600 rpm stirring for 3 hours.

The reaction can be followed directly from the color changes. The initial solution was pink due to the tetrazine color and gradually changed to orange and finally yellow (Fig. 1). In absence of gold salt, no color change was visible during the first two hours. However, when the reaction mixture was kept for a longer time (typically overnight), a pale yellow color can be observed at the end (Fig. S1†). These results are consistent with the possible reduction of the tetrazine by the thiol, responsible for the color changes.

A.2 Electron microscopy (TEM, SEM). The first characterization of the solution content at the end of the reaction was performed by transmission electronic microscopy (Fig. 2 and S2†).

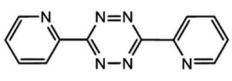

bptz

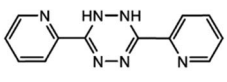

H_2bptz

Scheme 1 Formulae of bptz and its reduced form H_2bptz.

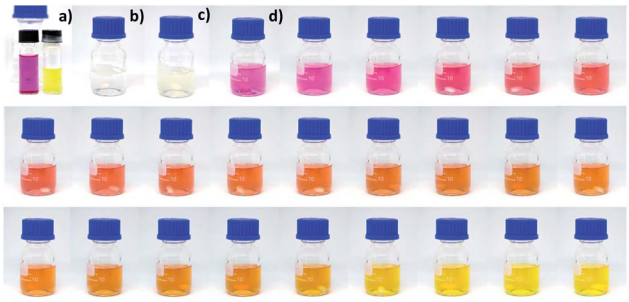

Fig. 1 Color changes during the synthesis: (a) initial (left) and final (right) reactional mixtures; (b) DDT; (c) DDT + $HAuCl_4$; (d) DDT + $HAuCl_4$ + bptz and following pictures taken every 7 minutes over a period of 160 minutes.

Gold NCs can be seen on TEM images taken on the final solution (Fig. 2A) without any purification. Many nano-objects with average diameter close to 2 nm can be seen in this sample. Other snapshots showing other areas can also be seen in Fig. S2† and confirm that a polydispersity in sizes and shapes does exist in this crude sample. The presence of Au NCs is strongly dependent on the proportions of reactants in the initial mixture, as shown in Fig. S3† where NCs are visible but mixed with large nanoparticles resulting from the aggregation of smaller ones. This point will be discussed in more details later on (Section B).

Centrifugation was performed to get rid of the large aggregated particles. After centrifugation, HRTEM pictures were taken confirming that NCs are still present in the supernatant with a rather narrow diameter range centered around 2 nm (Fig. 2B). Further purification was achieved by HPLC (see Section A.6 for details) and the purified clusters can be seen in Fig. 2C albeit in smaller amount than previously.

TEM images show that Au NCs are directly obtained in a one pot synthesis by simply mixing the gold salt, thiol and tetrazine in adequate proportions. In absence of bptz, the mixture DDT + $HAuCl_4$ does not lead to nanoclusters but to spherical nanoparticles with a diameter close to 20 nm (Fig. 3).

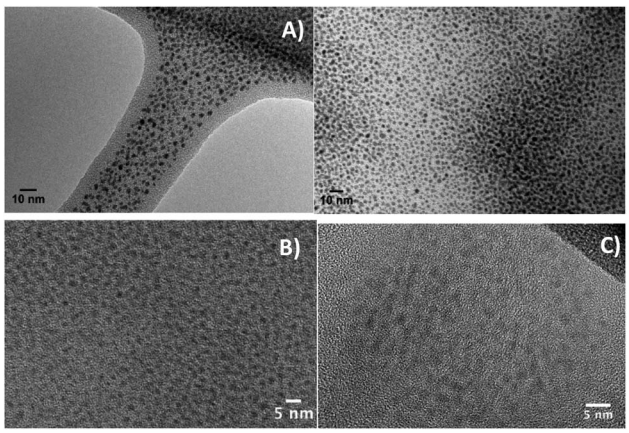

Fig. 2 (A) TEM snapshots (two different areas) of a crude sample directly after synthesis without purification; (B) HRTEM snapshot of the supernatant after purification by centrifugation. (C) HRTEM snapshot of the fraction isolated by HPLC.

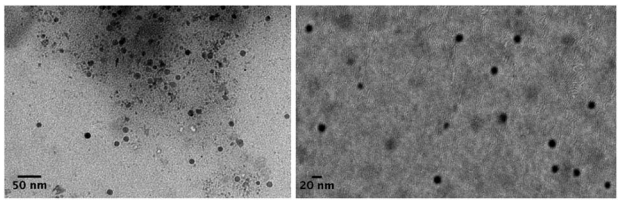

Fig. 3 TEM pictures at different magnifications of Au NPs obtained from the mixture of DDT and $HAuCl_4$ in ethanol, in absence of bptz.

SEM-EDS (Energy Dispersive Spectroscopy) was also performed on silicon substrates coated with nanoclusters after an additional washing of the precipitate in acetone to remove most of the unreacted thiols (see ESI for experimental details†). The results are shown in Fig. S4† for two different zones and demonstrate the simultaneous presence of Au, S and N elements, with atomic percentages of respectively 3.1, 26.4 and 27.6% for area 1 and 8.1, 23.4 and 14.4% for area 2. This suggests that both the thiol and the tetrazine may take part to the gold nanocluster stabilization but does not constitute a clear evidence as a direct characterization of the gold clusters would be.

To investigate further the reaction mechanism and in particular the precise role of bptz in the formation of nanoclusters, a monitoring by spectrophotometry was then undertaken.

A.3 UV-vis absorption and emission spectroscopies. To elucidate the mechanism of Au NC formation, the synthesis was monitored first by UV-vis absorption spectroscopy. The samples for spectral analysis were prepared by quickly taking an aliquot of 30 μL from the reaction medium at the specified time. Each sample was diluted to 2 mL (in absolute ethanol) directly in the cuvette a few seconds before each measurement. The overall evolution shown in Fig. 4, is in agreement with the color changes displayed in Fig. 1. It can be observed that two bands gradually decrease in intensity while another one simultaneously grows with time. The two decreasing bands are assigned respectively to the π–π* (300 nm, high intensity) and n–π* (535 nm, low intensity) of bptz (tetrazine chromophore) which are common features among tetrazine derivatives.[30] The growing band which is present even in absence of gold can be assigned to the reduced form of bptz, which is expected to be H_2bptz (bis-(3,6)pyridinyl-dihydrotetrazine, see Scheme 1)[24] but a contribution of Au NCs in that near-UV range cannot be excluded. Indeed, when the amount of Au is increased, the ratio between this band and the two other ones increases as well, while replacing Au by Ag has the opposite effect (see Fig. S5†).

The reaction kinetics can be investigated by UV-vis absorption as well (Fig. S6†). Beyond 15 minutes, the absorbance variation is very similar at 294 and 540 nm. These absorbance values decrease until approximately 120 minutes. This shows that bptz is gradually consumed upon time by the remaining DDT. The absorbance at 375 nm increases symmetrically on this time interval. We can thus conclude that the formation of Au NCs occurs mainly in the first ten minutes, because during this period the amount of bptz is supposed to remain nearly constant.

Contrarily to Au NPs, which can be easily characterized using UV-Vis absorption through their plasmon resonance bands, Au NCs do not exhibit any absorption in the visible and in UV the absorption of thiols and H_2bptz are likely to overlap the one of Au NCs. Therefore, we moved to emission spectroscopy measurements to characterize them. Fig. 5 displays the emission and excitation spectra of the final NC solution as well as the evolution of emission spectra with time during the synthesis.

Indeed, it has been already reported that Au NCs can be characterized by their emission properties upon irradiation in the UV interband.[31] An emission centered at 630 nm can be seen in our case (Fig. 5A) that appears since the initial mixture and increases slightly upon time (Fig. 5B). This red emission was already observed for various Au nanoclusters especially when stabilized by thiolates.[32,33] The excitation spectrum associated with this red emission actually comes from the band centered at 375 nm (see Fig. 5A), confirming the contribution of gold in this emission band. Moreover, in absence of gold, no emission was observed in that range (Fig. S7A†). Another band centered at 460 nm is also visible in the emission spectra of Au NCs (and absent as well without gold salt addition) but this one does not grow linearly with time. It is likely that aggregation processes may occur between individual NCs that might be at the origin of this significantly shorter wavelength emission, as it is reported that increasing the gold core size shifts the emission to higher energy values.[34]

The emission spectra of NCs can also be used to check the ability of various solvents to extract the Au NCs from the precipitate after centrifugation, to avoid too much loss in the

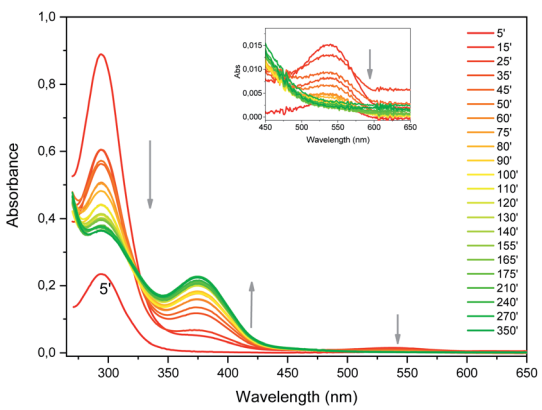

Fig. 4 UV-vis absorption spectra evolution upon synthesis of Au NCs (reaction time in minutes). Inset shows the magnification of the high wavelength region.

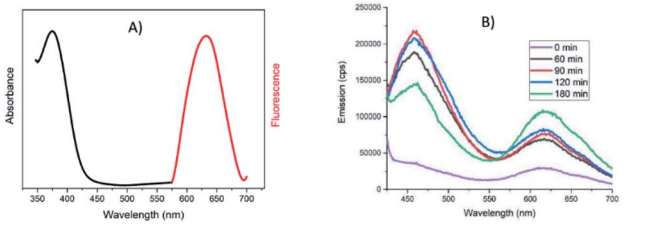

Fig. 5 (A) Emission (λ^{exc} = 368 nm, red trace) and excitation (λ^{em} = 630 nm, black trace) spectra of the final solution of clusters in ethanol; (B) Emission spectra (λ^{exc} = 368 nm) at various reaction times from 0 to 180 minutes.

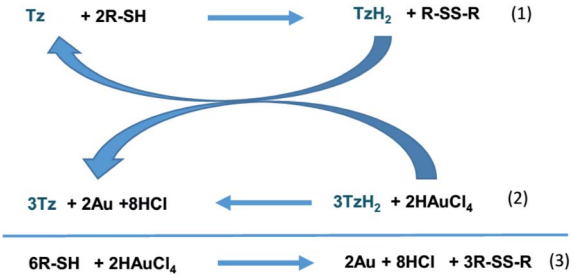

Scheme 2 Mechanism of Au NC formation starting from tetrazine (Tz) and alkanethiol (R-SH) and global outcome.

purification process. Among the solvents tested (chloroform, propanol, THF, toluene), chloroform seems to be the best for the extraction of Au NCs based on the intensity of the emission band at 630 nm (Fig. S7B†). As the stabilization of Au NCs by DDT ligands should decrease the polarity of these nano-objects, a less polar medium than the initial one is better suited for extraction, but the results show that the more apolar solvent (toluene) is not the best choice.

Based on these spectroscopic data, the following mechanism for Au NCs synthesis can be proposed (Scheme 2).

It was already reported that thiols can reduce bptz into H_2bptz and disulfide.[24] Therefore, it seems reasonable that the first step of the mechanism involves the reduction of bptz by DDT producing H_2bptz according to eqn (1). Then bptzH_2 can reduce Au(III) into Au(0) restoring bptz (eqn (2)). When DDT is in large excess, once Au(III) is totally consumed, the remaining thiol slowly reduces bptz into H_2bptz and disulfide, so that at the end all the tetrazine has been consumed by the first step. In that case, the outcome can be written according to eqn (3). Furthermore, part of the thiol in excess is used to stop the Au(0) growth at early stage leading to Au NCs.

Based on the postulated mechanism in Scheme 2, it should be possible to obtain Au(0) by the direct reduction of Au(III) by thiols in ethanol in absence of Tz. This is actually the case and evidenced by emission spectroscopy (see Fig. S8†). Indeed, a similar trend in the emission intensity recorded at 630 nm under UV excitation is observed for the binary Au(III)–DDT mixture compared to the ternary Au(III)–DDT–bptz mixture, while all other compositions do not give any significant emission and in all cases this residual emission remains constant. However, the final state is different, since mainly nanoparticles of 20 nm diameter can be seen when the reaction is conducted in absence of bptz (Fig. 3). Thus it can be deduced that bptz plays a critical role in the formation of NCs.

A.4 Mass spectrometry (MS). MALDI-MS was performed on as-synthesized AuNCs (see Fig. 6). Experimental conditions for these measurements can be found in ESI.† In that ionization mode, we were not able to identify the original clusters, nevertheless characteristic fragments can be clearly assigned in the spectra, like $Au_5(DDT)_5$ at *m*/*z* 1995, $Au_6(DDT)_5$ at *m*/*z* 2187, $Au_6(DDT)_7$ at *m*/*z* 2589 or $Au_7(DDT)_8$ at *m*/*z* 2983. The isotopic pattern is also consistent with the presence of gold.

A.5 XPS. The XPS spectra are shown in Fig. S9† and the main results summarized in Table 1.

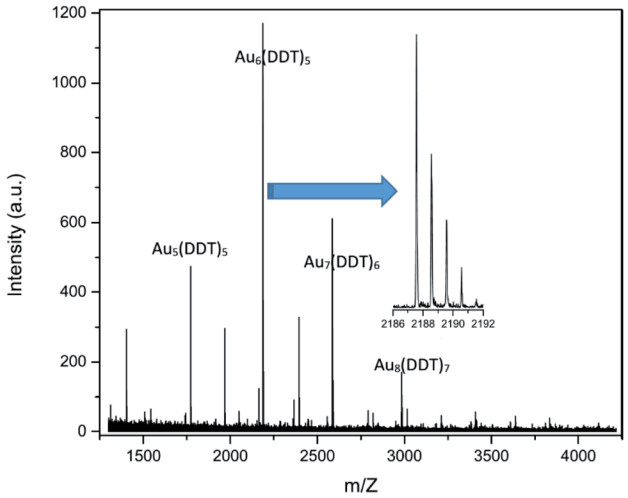

Fig. 6 MALDI-TOF mass spectrum of the Au NC sample just after synthesis. No peaks have been observed at higher *m*/*z* values.

The Au(4f) signal shows two characteristic peaks as expected for Au NCs,[35] corresponding to ($4f_{5/2}$) for the high energy one and ($4f_{7/2}$) for the low energy one. The Au($4f_{7/2}$) signal peaking at 83.98 eV corresponds to an energy very close to that of metallic gold (83.9 eV) as it is usually the case in Au NCs.[35] The sulphur signal at 162.5 eV and the carbon signal at 284.4 eV are perfectly in the range expected for alkyl thiolates.[36] All these data confirm the presence of Au NCs stabilized by dodecanethiolates.

The main unexpected result is the very low amount of nitrogen in the composition of clusters derived from XPS. This seems in contradiction with the results of SEM-EDS (see Fig. S4† and discussion above) showing the simultaneous presence of Au, S and N in the same area. This can be nevertheless rationalized by the fact that tetrazines can be easily sublimated[30,37] and are thus likely to be removed under the high vacuum conditions required for XPS analysis.

A.6 Purification by HPLC. After centrifugation, a further purification step was performed using HPLC to try to separate the unreacted molecular species from NCs.

A first HPLC analytical isolation was conducted by using a Phenomenex Luna C-12 column with an isocratic flow of methanol and water (80 : 20, 1 mL min^{-1}). The filtered mother solution was concentrated at room temperature under vacuum before injection; only ethanol was removed. In this case, the analytical HPLC was used as preparative HPLC using an injection loop of 5 μL to collect the different fractions in order to

Table 1 Composition of the Au NC sample drop cast on a silicon wafer deduced from XPS spectra

Element	Peak bond energy/eV	Atomic%
Au 4f	83.98	5.05
C 1s	284.43	85.32
N 1s	399.27	0.46
O 1s	532.03	3.78
S 2p	162.51	5.39
Si 2p	98.96	0

limit the influence of the co-elution of DDT and obtain the maximum of peak intensity at 290 nm. Each sample was analyzed under a pressure of 100 to 110 bar (more detailed conditions in ESI†).

The results are displayed in Fig. 7 and S10.† First it can be seen that bptz and DDT actually react together from the disappearance of the peak at a retention time (t_R) ≈3.5 minutes in the mixture and the appearance of a new peak at $t_R = 4.4$ min (Fig. S10†). This latter is also visible for the ternary mixture, along with another small one just behind. A small peak at 3.2 minutes can also be seen in the ternary mixture that corresponds to the one observed in the sample containing DDT only. This result is consistent with the fact that the thiol is in large excess and is supposed to remain in the final mixture once the reaction is over.

In order to optimize the peak separation, a second optimization was performed using a Phenomenex Luna C-18 column with analytical HPLC equipped with an injection loop of 20 µL and an isocratic flow of MeOH : H_2O mixture with a ratio of 50 : 50 to get a pressure of 100–110 bar during the separation process. The comparison of the chromatogram in Fig. 7 with the one of Fig. S10† shows that the peak order is similar as with the previous conditions, and that the AuNCs peak appears after the one of H_2bpTz, at $t_R \approx 21$ min. Due to the low concentration of obtained clusters in this solvent, the fraction corresponding to isolated AuNCs obtained at $t_R \approx 21$ min is colorless. As shown in Fig. 7, the comparison of the Au NC sample with another one without gold unambiguously confirms the assignment of the 21st minute peak to the Au NCs.

To collect enough amounts for further characterizations such as for HRTEM, the method was then transposed on a semi-preparative HPLC. The collection was realized at 20 °C, with a 200 µL injection loop, a Phenomenex Luna C-18 (250 × 10 mm, 5 µm, 100 Å), with an isocratic flow of EtOH : H_2O (40 : 60, 3 mL min^{-1}). In such conditions (Fig. S11†), the final isolated clusters were collected for a $t_R \approx 20$ to 22 minutes at 190 nm. Au NCs are actually present in this fraction as they can be directly seen in the HRTEM snapshots of Fig. 2C.

A.7 NMR. Finally, NMR was performed to try to identify more precisely which ligand is actually present at the surface of NCs. Indeed, while it is well known that thiols are efficient ligands to stabilize gold nano-objects, tetrazine compounds were also reported as possible candidates for that role[23] but the great excess of thiols and a stronger Au–S interaction might prevent tetrazine from being present at the Au cluster surface.

Fig. 8 shows the high chemical field region of ^{1}H and ^{13}C NMR spectra recorded for bptz, the bptz + DDT mixture (thus involving H_2bptz) and the Au NC fraction isolated from HPLC. All these spectra clearly display the signals assigned to the 4 pyridine hydrogen atoms (colored dots), but at different chemical shifts. Hydrogen resonances are shifted upfield from bptz to the binary mixture H_2bptz, in agreement with the presence of the hydrogen on the dihydrotetrazine ring, which should attract the electron density of the pyridine nitrogen.

Interestingly, these four characteristic signals are also clearly identified in the NC ^{1}H spectra (Fig. S12†), while ungrafted tetrazine is supposed to have been removed upon HPLC separation. Fig. S12† shows the entire spectrum as well, with the characteristic resonance peaks assigned to the hydrogen atoms of the DDT alkyl chain in the 0.5–3 ppm range. A shift of the

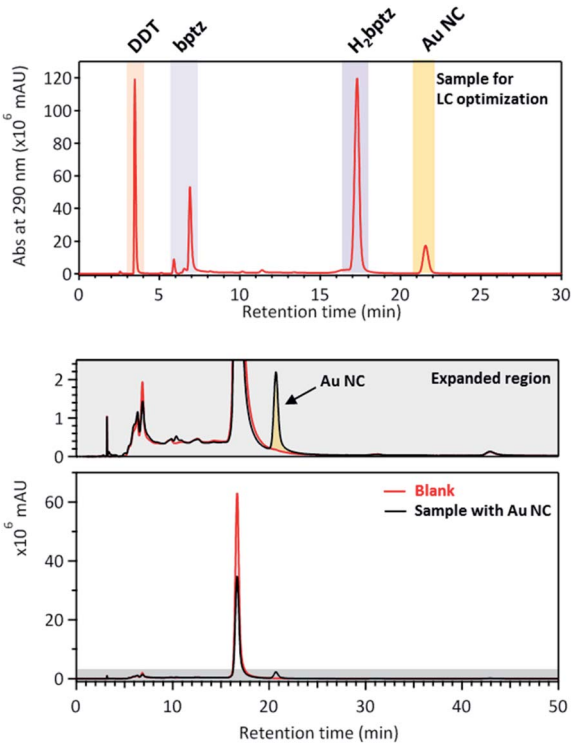

Fig. 7 HPLC chromatograms of the sample containing Au NCs (top), and the comparison of another Au NC sample with a blank sample containing no gold (bottom). Conditions: MeOH : H_2O (50 : 50), Phenomenex Luna C-18, 1 mL min^{-1}, 110 bar.

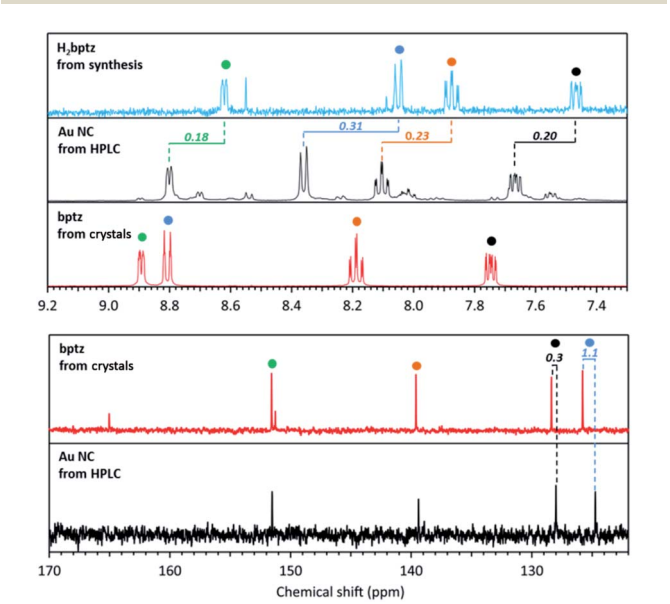

Fig. 8 ^{1}H (top) and ^{13}C (bottom) NMR spectra in MeOD of Au NCs isolated from HPLC (black line), bptz + DDT mixture leading to H_2bptz (blue line) and bptz from crystal (red line).

Table 2 Proportions of bptz, Au salt and DDT in the samples investigated. The common amount of bptz is 25 μmol in 2.5 mL of ethanol[a]

Sample	bptz : Au : DDT
1	1 : 0.5 : 25
2	1 : 2 : 2
3	1 : 1 : 2
4	1 : 0.25 : 2
5	1 : 0.25 : 25

[a] For comparison, the bptz : Au : DDT ratio is 1 : 0.2 : 500 for the NCs synthesized in Section A.

chemical shift values of the methylene protons can be observed between the Au NC sample and the one without Au, due to the participation of the DDT ligand in the stabilization of Au, while the terminal methyl remains unaffected.

Fig. S13† shows the ^{13}C resonance peaks due to tetrazine and thiol, which demonstrates that Au NCs are stabilized by both ligands although tetrazine signals were not observed in MS or in XPS. When comparing the chemical shifts of ^{1}H and ^{13}C spectra, an upfield effect is also observed between bptz and NCs. A possible explanation is the interaction between N and Au in the NCs leading to the same trend in the resonance positions of the hydrogens of the pyridine ring, but with a weaker effect (−0.10 *vs.* −0.30 ppm on average, see Table S1†), Au being less electropositive than H.

We can thus conclude definitively that DDT and bptz play both the role of ligand of Au nanoclusters.

B. Au nanoparticles

B.1 Synthesis. The synthesis of Au NCs is enabled by the large amount of DDT available to stabilize Au(0) at early stages of the nucleation-growth process and avoid aggregation into larger particles. Decreasing this amount is expected to lead to nanoparticles (NPs) and to check that point, new syntheses with a similar protocol as in Section A.1 but radically different proportions between Au, bptz and DDT were tested (see Table 2 for composition details).

B.2 Electronic microscopy. The results at the end are very different according to the proportions used and in particular to the relative amount of thiol *vs.* Au and bptz. For sample 2, Fig. 9 shows that Au NCs are still visible but Au NPs in the 10 nm range are formed as well and tend to coalesce into larger aggregated nano-objects with a nanodendritic shape, having diameters over 50 nm. Similar observations were found for sample 3 (Fig. S3†). This morphology change from NCs to NPs and assemblies of NPs is related to the higher Au : S ratio making the amount of unreacted thiol not enough to stabilize clusters just after the nucleation step and the growth step is not blocked anymore. These nanodendritic assemblies of nanoparticles might be of interest for applications requiring high developed areas like catalysis.

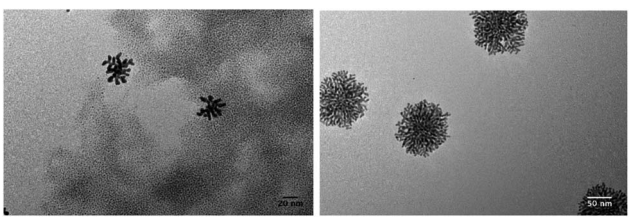

Fig. 9 TEM pictures of Au NPs synthesized for sample 2 (see Table 1).

B.3 UV-vis absorption. The UV-vis absorption monitoring is instructive to understand the growth mechanism (see Fig. 10A). The measurements were done similarly to the investigation of Au NCs described above (see Section A.3). No absorption corresponding to bptz can be observed in the early reaction times, neither the band at 300 nm assigned to the π–π* transition nor the band at 540 nm assigned to the n-π* transition. After 30 minutes, the absorption bands corresponding to bptz start to appear again. Simultaneously the UV band at 227 nm which can be assigned to thiol gradually drops. We can thus consider that the process does not consume the tetrazine, which is consistent with the postulated mechanism (Scheme 2) because reaction (1) cannot terminate the process anymore. Looking closer to the spectral evolution tends to show that at the longest reaction times, the bptz absorption bands grow again while the thiol has been fully consumed and no more Au NPs are formed. This means that another reaction than (2) can contribute to the formation of bptz. We may assume that dissolved oxygen can play the role of oxidant of H_2bptz, leading to the regeneration of bptz without additional Au.

Changing the proportions of Au *vs.* DDT allows moving from Au NCs to Au NPs and this can be directly seen in UV-vis

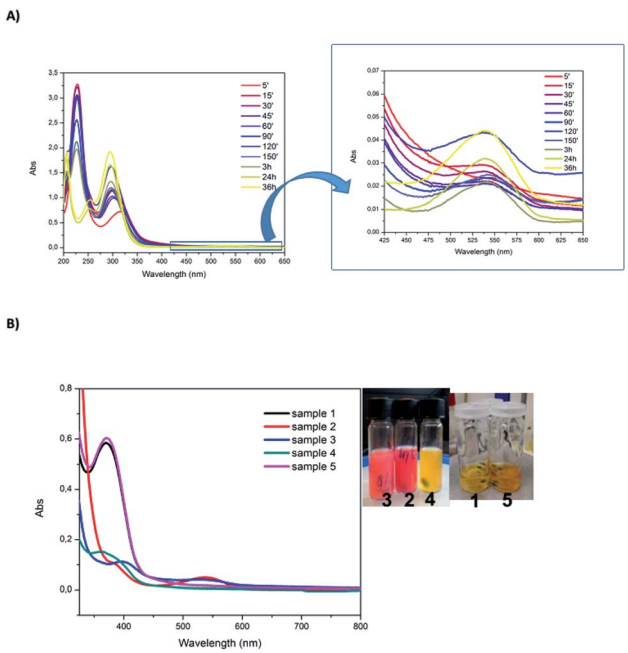

Fig. 10 (A) UV-vis absorption monitoring of the reaction with the following proportions of reactants: Au : bptz : DDT 1 : 1 : 2 (sample 2 in Table 1). Times in minutes. (B) UV-vis absorption spectra after 5 minutes of reaction and pictures at end of the reaction for the five samples (see Table 1 for the proportions corresponding to each sample).

absorption spectra (Fig. 10B). The main difference is the presence of a plasmon resonance band at 540 nm when Au NPs are produced (samples 2 and 3) while no absorption band in the visible range can be seen for Au NCs (samples 1, 4 and 5). Therefore, the solution color moves from light yellow for Au NCs to reddish for Au NP. Moreover, the band located at 380 nm is also indicative of Au NCs as noticed previously (although mixed with the absorption of H_2bptz). Samples 1 and 5 display the largest intensity at that wavelength, while for sample 2 the intensity is the lowest. In sample 4, as the amount of Au is low, the concentration of Au NPs might remain low and the reoxidation of H_2bptz by $HAuCl_4$ remains limited, explaining the high absorption in the near UV range. Thus we can conclude that a direct relation exists between the Au : DDT ratio and the formation of Au NCs *vs.* Au NP on one hand, and the intensity of the nearest UV band on the other hand which also depends on the bptz:Au ratio.

Conclusions

Gold nanoclusters have been synthesized in a one-pot reaction in ethanol using a reductant generated *in situ* by the reduction of a tetrazine derivative by a thiol. Well-calibrated clusters with diameters slightly below 2 nm were obtained after centrifugation when a large excess of thiols was used. The tetrazine is necessary to get nanoclusters only since the direct reaction of gold salt with dodecanethiol leads mainly to nanoparticles. Changing the proportions of gold *vs.* thiol allows one to move from Au nanoclusters to Au nanoparticles that assemble into aggregates of 50 nm diameter. UV-vis spectrophotometry can be used to monitor the reaction and have insight in the mechanism. While the tetrazine is fully consumed when the reaction is over in the case of clusters, the limiting reactant is the thiol in the case of particles. Fluorescence spectroscopy can be used to characterize the nanoclusters by their emission at 630 nm when excited in UV. HPLC allows one to purify the clusters by removing all the unreacted molecular species. Finally, NMR analysis shows that the tetrazine is still present in the fraction containing only the clusters with chemical shifts different from the isolated compound, demonstrating that some tetrazines serve as ligands on the cluster surface. Ongoing investigations now focus on supporting these gold nanoclusters on carbonaceous materials like reduced graphene oxide to design new nanomaterials active in heterogeneous catalysis.

Conflicts of interest

There are no conflicts to declare.

Acknowledgements

Y. B. Rus acknowledges the Indonesia Endowment Fund for Education (LPDP) scholarship for funding his thesis. P. Decorse (ITODYS, Université de Paris) is acknowledged for XPS spectra.

Notes and references

1 V. A. Ogarev, V. M. Rudoi and O. V. Dement'eva, *Inorg. Mater. Appl. Res.*, 2018, **9**, 134–140.
2 Y.-C. Yeh, B. Creran and V. M. Rotello, *Nanoscale*, 2012, **4**, 1871–1880.
3 E. Boisselier and D. Astruc, *Chem. Soc. Rev.*, 2009, **38**, 1759–1782.
4 K. Saha, S. S. Agasti, C. Kim, X. Li and V. M. Rotello, *Chem. Rev.*, 2012, **112**, 2739–2779.
5 A. Corma and H. Garcia, *Chem. Soc. Rev.*, 2008, **37**, 2096–2126.
6 J. Turkevich, *Discuss. Faraday Soc.*, 1951, **11**, 55.
7 M. Brust, M. Walker, D. Bethell, D. J. Schiffrin and R. Whyman, *J. Chem. Soc., Chem. Commun.*, 1994, 801–802.
8 R. H. Terrill, T. A. Postlethwaite, C. H. Chen, C. D. Poon, A. Terzis, A. D. Chen, J. E. Hutchison, M. R. Clark, G. Wignall, J. D. Londono, R. Superfine, M. Falvo, C. S. Johnson, E. T. Samulski and R. W. Murray, *J. Am. Chem. Soc.*, 1995, **117**, 12537–12548.
9 R. C. Jin, *Nanoscale*, 2010, **2**, 343–362.
10 Y. Lu and W. Chen, in *Gold Clusters, Colloids and Nanoparticles I*, ed. D. M. P. Mingos, Springer International Publishing, Cham, 2014, pp. 117–153, DOI: 10.1007/430_2013_126.
11 M. J. Hostetler, J. E. Wingate, C. J. Zhong, J. E. Harris, R. W. Vachet, M. R. Clark, J. D. Londono, S. J. Green, J. J. Stokes, G. D. Wignall, G. L. Glish, M. D. Porter, N. D. Evans and R. W. Murray, *Langmuir*, 1998, **14**, 17–30.
12 X. C. Qu, Y. C. Li, L. Li, Y. R. Wang, J. N. Liang and J. M. Liang, *J. Nanomater.*, 2015, 784097.
13 Y. Bao, C. Zhong, D. M. Vu, J. P. Temirov, R. B. Dyer and J. S. Martinez, *J. Phys. Chem. C*, 2007, **111**, 12194–12198.
14 J. Lin, Z. Zhou, Z. Li, C. Zhang, X. Wang, K. Wang, G. Gao, P. Huang and D. Cui, *Nanoscale Res. Lett.*, 2013, **8**, 170.
15 Z. Wu, J. Suhan and R. C. Jin, *J. Mater. Chem.*, 2009, **19**, 622–626.
16 T. Huang, L. Huang, Y. Jiang, F. C. Hu, Z. H. Sun, G. Q. Pan and S. Q. Wei, *Dalton Trans.*, 2017, **46**, 12239–12244.
17 N. K. Pal and C. Kryschi, *J. Nanopart. Res.*, 2015, **17**, 226.
18 N. K. Pal and C. Kryschi, *Phys. Chem. Chem. Phys.*, 2015, **17**, 21423–21431.
19 N. K. Chaki, P. Singh, C. V. Dharmadhikari and K. P. Vijayamohanan, *Langmuir*, 2004, **20**, 10208–10217.
20 W. W. Weare, S. M. Reed, M. G. Warner and J. E. Hutchison, *J. Am. Chem. Soc.*, 2000, **122**, 12890–12891.
21 J. Lin, Z. J. Zhou, Z. M. Li, C. L. Zhang, X. S. Wang, K. Wang, G. Gao, P. Huang and D. X. Cui, *Nanoscale Res. Lett.*, 2013, **8**, 170.
22 R. Zhou, M. Shi, X. Chen, M. Wang and H. Chen, *Chem.–Eur. J.*, 2009, **15**, 4944–4951.
23 S. Samanta, S. Das and P. Biswas, *Sens. Actuators, B*, 2014, **202**, 23–30.
24 S. Samanta, S. Ray, A. B. Ghosh and P. Biswas, *RSC Adv.*, 2016, **6**, 39356–39363.

25 M. L. Blackman, M. Royzen and J. M. Fox, *J. Am. Chem. Soc.*, 2008, **130**, 13518–13519.
26 Y. Li, F. Miomandre, G. Clavier, L. Galmiche, V. Alain-Rizzo and P. Audebert, *ChemElectroChem*, 2017, **4**, 430–435.
27 K. Neumann, S. Jain, J. Geng and M. Bradley, *Chem. Commun.*, 2016, **52**, 11223–11226.
28 R. Aufaure, J. Hardouin, N. Millot, L. Motte, Y. Lalatonne and E. Guenin, *Chem.–Eur. J.*, 2016, **22**, 16022–16027.
29 J. Zhu, J. Hiltz, R. B. Lennox and R. Schirrmacher, *Chem. Commun.*, 2013, **49**, 10275–10277.
30 G. Clavier and P. Audebert, *Chem. Rev.*, 2010, **110**, 3299–3314.
31 L.-Y. Chen, C.-W. Wang, Z. Yuan and H.-T. Chang, *Anal. Chem.*, 2015, **87**, 216–229.
32 J. Xie, Y. Zheng and J. Y. Ying, *J. Am. Chem. Soc.*, 2009, **131**, 888.
33 L. Jin, Y. Fang, L. Shang, Y. Liu, J. Li, L. Wang, P. Hu and S. Dong, *Chem. Commun.*, 2013, **49**, 243–245.
34 T.-Q. Yang, B. Peng, B.-Q. Shan, Y.-X. Zong, J.-G. Jiang, P. Wu and K. Zhang, *Nanomaterials*, 2020, **10**, 261.
35 P. Zhang, *J. Phys. Chem. C*, 2014, **118**, 25291–25299.
36 S. Ge, J. Zhao and G. Ma, *Inorg. Chem. Commun.*, 2019, **109**, 107556.
37 D. Wang, W. Chen, Y. Zheng, C. Dai, L. Wang and B. Wang, *Heterocycl. Commun.*, 2013, **19**, 171–177.